Downregulation of Adipose Glutathione S-Transferase A4 Leads to Increased Protein Carbonylation, Oxidative Stress, and Mitochondrial Dysfunction

Jessica M. Curtis,[1] Paul A. Grimsrud,[1] Wendy S. Wright,[1] Xin Xu,[2] Rocio E. Foncea,[1] David W. Graham,[1] Jonathan R. Brestoff,[1] Brian M. Wiczer,[1] Olga Ilkayeva,[3] Katherine Cianflone,[4] Deborah E. Muoio,[3,5] Edgar A. Arriaga,[2] and David A. Bernlohr[1]

OBJECTIVE—Peripheral insulin resistance is linked to an increase in reactive oxygen species (ROS), leading in part to the production of reactive lipid aldehydes that modify the side chains of protein amino acids in a reaction termed protein carbonylation. The primary enzymatic method for lipid aldehyde detoxification is via glutathione S-transferase A4 (GSTA4) dependent glutathionylation. The objective of this study was to evaluate the expression of GSTA4 and the role(s) of protein carbonylation in adipocyte function.

RESEARCH DESIGN AND METHODS—GSTA4-silenced 3T3-L1 adipocytes and GSTA4-null mice were evaluated for metabolic processes, mitochondrial function, and reactive oxygen species production. GSTA4 expression in human obesity was evaluated using microarray analysis.

RESULTS—GSTA4 expression is selectively downregulated in adipose tissue of obese insulin-resistant C57BL/6J mice and in human obesity-linked insulin resistance. Tumor necrosis factor-α treatment of 3T3-L1 adipocytes decreased GSTA4 expression, and silencing GSTA4 mRNA in cultured adipocytes resulted in increased protein carbonylation, increased mitochondrial ROS, dysfunctional state 3 respiration, and altered glucose transport and lipolysis. Mitochondrial function in adipocytes of lean or obese GSTA4-null mice was significantly compromised compared with wild-type controls and was accompanied by an increase in superoxide anion.

CONCLUSIONS—These results indicate that downregulation of GSTA4 in adipose tissue leads to increased protein carbonylation, ROS production, and mitochondrial dysfunction and may contribute to the development of insulin resistance and type 2 diabetes. ***Diabetes*** **59:1132–1142, 2010**

From the [1]Department of Biochemistry, Molecular Biology and Biophysics, The University of Minnesota, Minneapolis, Minnesota; the [2]Department of Chemistry, The University of Minnesota, Minneapolis, Minnesota; the [3]Sarah W. Stedman Nutrition and Metabolism Center, Duke University, Durham, North Carolina; the [4]McGill University Health Centre, Montreal, Canada; and the [5]Departments of Medicine and Pharmacology & Cancer Biology, Duke University, Durham, North Carolina.

Corresponding author: David A. Bernlohr, bernl001@umn.edu.

Received 28 July 2009 and accepted 27 January 2010. Published ahead of print at http://diabetes.diabetesjournals.org on 11 February 2010. DOI: 10.2337/db09-1105.

J.M.C., P.A.G., and W.S.W. contributed equally to this study.

Obesity-linked type 2 diabetes and its associated health complications are major human health concerns (1), and recent studies have implicated increased levels of reactive oxygen species (ROS) such as superoxide anion, hydrogen peroxide, peroxynitrite, and hydroxyl radicals as major contributing factors (2–4). Excess ROS are causally linked to insulin resistance in adipocytes (5) and alteration of adipokine secretion in a manner that promotes insulin resistance in peripheral tissues (2,6,7). As adipose metabolism plays a substantial role in regulating whole-body insulin sensitivity (8), evaluating the conditions that lead to oxidative stress in adipocytes is an important goal.

Whereas various ROS react with all cellular components, the hydroxyl radical–mediated peroxidation of polyunsaturated acyl chains of glycerophospholipids is particularly harmful as it results in the formation of lipid peroxidation products considered second messengers of oxidative stress (9). Peroxidated acyl chains are unstable and undergo nonenzymatic Hock cleavage generating a family of reactive α,β-unsaturated aldehydes (10). Such reactive lipid aldehydes, including *trans*-4-hydroxy-2-nonenal (4-HNE), covalently modify protein and DNA and activate cellular stress-response systems (11) and the transcription factors Nrf2 and Tfam (12,13). In the case of protein modification, the process is generically termed protein carbonylation and often results in loss of function (14).

Using proteomic profiling, we have previously shown that high-fat–fed obese, glucose-intolerant C57BL/6J mice exhibit approximately twofold to threefold increased adipose protein carbonylation compared with lean controls (15). In addition, obese animals exhibited an approximately fourfold decrease in the abundance of glutathione S-transferase A4 (GSTA4) in adipose tissue. GSTA4 catalyzes the glutathionylation of α,β-unsaturated aldehydes to produce a conjugation product that is transported from the cell (16). Our studies here focus on the role of GSTA4 as an antioxidant enzyme linking protein carbonylation to metabolic dysfunction. We reveal that GSTA4 is downregulated specifically in adipose tissue of obese mice, insulin-resistant humans, and also in 3T3-L1 adipocytes treated with tumor necrosis factor (TNF)-α. Mitochondria from both GSTA4-silenced 3T3-L1 adipocytes and adipose tissue of GSTA4-null or obese C57BL/6J mice accumulate ROS and exhibit compromised respiration. Metabolically, this results in impaired glucose and lipid homeostasis, suggesting that TNF-α–induced downregulation of GSTA4

is a major determinant linking inflammation with oxidative stress and insulin resistance.

RESEARCH DESIGN AND METHODS

Animals. C57BL/6J mice were placed on a normal chow (~4% fat by weight; Teklad) or a high-fat (~35% fat by weight, F3282; BioServ) diet at weaning (17). Mice were housed on a 12-h light/dark cycle and fed ad libitum with continual access to water. At 12–16 weeks of age, mice were killed by cervical dislocation, and tissues were harvested, frozen in liquid nitrogen, and stored at −80°C until further processing. Primary adipocytes were isolated from fresh epididymal fat pads as described previously (18). Mixed-strain mice B6;129S5-GSTa4$^{Gt(neo)\ 619\ Lex}$ were purchased from the Mutant Mouse Regional Resource Centers (University of California-Davis, Davis, CA). GSTA4 heterozygous mice were outbred to C57/BL6J mice, and the resulting heterozygous progenies were interbred to generate GSTA4-null and wild-type mice. The University of Minnesota Institutional Animal Care and Use Committee approved all experiments.

Generation of GSTA4-silenced adipocytes. The 3T3-L1 fibroblasts were transduced with lentivirus carrying short hairpin RNA (shRNA) as described previously (19). shRNA sequences directed toward GSTA4 mRNA were purchased from Ambion. Each oligo and the reverse complement were synthesized and annealed, and the double-stranded DNA was ligated into pENTR/U6 cloning vector (Invitrogen) according to manufacturer's protocol. Cell lines used for experiments contained the following shRNA sequences: scrambled (Scr) control, AGTACTGCTTACGATACGGTGTGCTGTCCGTAT CGTAAGCAGTACT; GSTAA4 knockdown, GGTATATAGATCCCAGGAGTGT GCTGTCCTCCTGGGATCTATATACC.

Protein carbonylation. Protein carbonylation was detected using EZ-link Biotin Hydrazide (Pierce) as described previously (15), with slight modifications. Polyvinylidene fluoride membranes (MilliPore, Billerica, MA) were blocked in Odyssey Blocking Buffer (LI-COR, Lincoln, NE), and biotinylated proteins were detected with DyLight 800–conjugated streptavidin (Pierce, Rockford, IL) and visualized using an Odyssey Infrared Imager (LI-COR).

Mitochondrial isolation, respiration, and matrix superoxide. 3T3-L1 adipocytes were scraped and incubated for 20 min on ice in 20 mmol/l Tris (pH 6.8) and 1 mmol/l EDTA containing protease inhibitors. Cells were lysed with 40 strokes of a Dounce homogenizer, and the resulting homogenate was supplemented with a final concentration of 220 mmol/l mannitol and 70 mmol/l sucrose. For mitochondrial isolation from adipose tissue, epididymal fat pads were minced, washed in ice-cold Krebs-Ringer HEPES, and lysed with 1:5 wt/vol of isolation buffer (20 mmol/l Tris-HCl, 220 mmol/l mannitol, 70 mmol/l sucrose, 1 mmol/l EDTA, pH 7.4, supplemented with protease inhibitors) by Dounce homogenization. Homogenates were centrifuged at 700*g* to remove nuclei, unbroken cells, and the lipid cake. Mitochondria were recovered by centrifugation at 12,000*g*.

Oxidative respiration was assessed in isolated mitochondria as described previously (20) using a FOXY-R Oxygen Sensor (Ocean Optics, Dunedin, FL). Isolated mitochondria were incubated at room temperature in 10 mmol/l HEPES (pH 7.4), 125 mmol/l KCl, 5 mmol/l $MgCl_2$, and 2 mmol/l K_2HPO_4 supplemented with 5 mmol/l pyruvate and 5 mmol/l malate to stimulate state 2 respiration. State 3 respiration was measured after the addition of 0.5 mmol/l ADP, and oxygen consumption rate was normalized to mitochondrial protein. TPP-HE was used to detect superoxide in isolated mitochondria as described previously (21).

Analysis of human GSTA4 expression. Microarray analysis of human genes expressed in omental and subcutaneous adipose tissue was reported by MacLaren et al. (22). Dataset analysis was conducted using the Significant Analysis of Microarrays procedure (23) version 3.02 available at http://www-stat.stanford.edu/~tibs/SAM. Statistical analyses were conducted using the statistical package SAS, version 9.1.3 (SAS Institute, Cary, NC).

Statistical analysis. All values are expressed as mean ± SEM. Statistical significance was determined using the two-tailed Student *t* test assuming unequal variances or, where appropriate, a two-way ANOVA with Bonferroni or Holm-Sidak post hoc analysis. P values < 0.05 are considered significant (*) with an increased significance of P value < 0.01 indicated (**).

RESULTS

To evaluate the expression of genes linked to oxidative stress and 4-HNE metabolism, quantitative RT-PCR (qPCR) (supplementary Table 1, available in an online appendix at http://diabetes.diabetesjournals.org/cgi/content/full/db09-1105/DC1) was performed on mRNA isolated from gonadal white adipose tissue of lean or obese male C57BL/6J mice (Fig. 1*A*). Adipose tissue from obese animals exhibited increased expression of p40 phox subunit of NADPH oxidase and heme oxygenase (HO-1) and trends toward increased expression of superoxide dismutase 1 (SOD-1), glutathione peroxidase 1 (GPX-1), and peroxyredoxin 1 (PRDX-1), all consistent with an antioxidant stress response (2). In contrast, the expression of multiple isoforms of the GST family (A4, A3, M2) was decreased in obese mice compared with lean controls. Most notably, the expression of GSTA4 decreased approximately threefold to fourfold, consistent with microarray analysis of lean and obese C57BL/6J mice in which GSTA4 expression was profiled among the most highly regulated transcripts (24). The expression of other 4-HNE metabolizing enzymes including several aldehyde dehydrogenases (ALDH1A 1/7, ALDH2, and FALDH) was not significantly altered with obesity (Fig. 1*A*). GSTA3 and GSTA4 expression was also decreased in obese female mice (Fig. 1*B*) relative to lean controls. Interestingly, the basal GSTA4 expression in adipose tissue of lean female mice was approximately twofold greater than in lean male mice, such that obese female mice express GSTA4 at levels comparable with that expressed by lean male animals (Fig. 1*B*).

To determine the tissue specificity of GSTA4 downregulation, qPCR was performed on mRNA isolated from epididymal white adipose tissue (EWAT), subcutaneous white adipose tissue, brown adipose tissue, liver, and gastrocnemius muscle of lean and obese male mice (Fig. 1*C*). Whereas decreased GSTA4 expression was observed in both visceral and subcutaneous white adipose tissue, no significant change was observed in other insulin-responsive tissues analyzed. Because adipose tissue contains multiple cell types, adipocytes were separated from stroma in EWAT by collagenase digestion and exhibited an ~95% decrease in GSTA4 expression in the adipocyte fraction. Reduced expression of GSTA4 was not limited to high-fat–fed C57BL/6J mice. GSTA4 mRNA expression was also significantly decreased in adipose tissue from *ob/ob* animals (Fig. 1*D*), and GSTA4 expression is downregulated ~10-fold in adipose tissue of genetically obese BTBR mice (http://www.diabetes.wisc.edu; [25]), indicating that the expression of GSTA4 is markedly reduced in a variety of metabolic and genetic models of obesity and insulin resistance.

GSTA4 expression in murine and human systems. To investigate the mechanism underlying reduced GSTA4 expression in insulin-resistant adipocytes, we assessed GSTA4 mRNA expression in response to a variety of hormones and metabolites using the 3T3-L1 cell culture system. Treatment of 3T3-L1 adipocytes with the proinflammatory cytokine TNF-α resulted in a time- and concentration-dependent decrease in GSTA4 expression. After 24-h treatment, GSTA4 mRNA expression was reduced 40% with 100 pmol/l TNF-α and 80% with 1 nmol/l TNF-α (Fig. 2*A*). No further reduction of GSTA4 expression was obtained with 10 nmol/l TNF-α (data not shown). The reduced GSTA4 expression was observed as early as 8 h with 1 nmol/l TNF-α treatment (Fig. 2*B*).

To assess the expression of GSTA4 in human obesity and insulin resistance, we evaluated GSTA4 expression in omental and subcutaneous adipose from obese diabetic subjects and nondiabetic subjects and compared it with lean counterparts using microarray analysis (22). Interestingly, GSTA4 expression in adipose tissue of humans was decreased in the obese insulin-resistant population relative to lean and obese insulin-sensitive individuals (Fig. 3*A*) and was verified using real-time PCR (results not

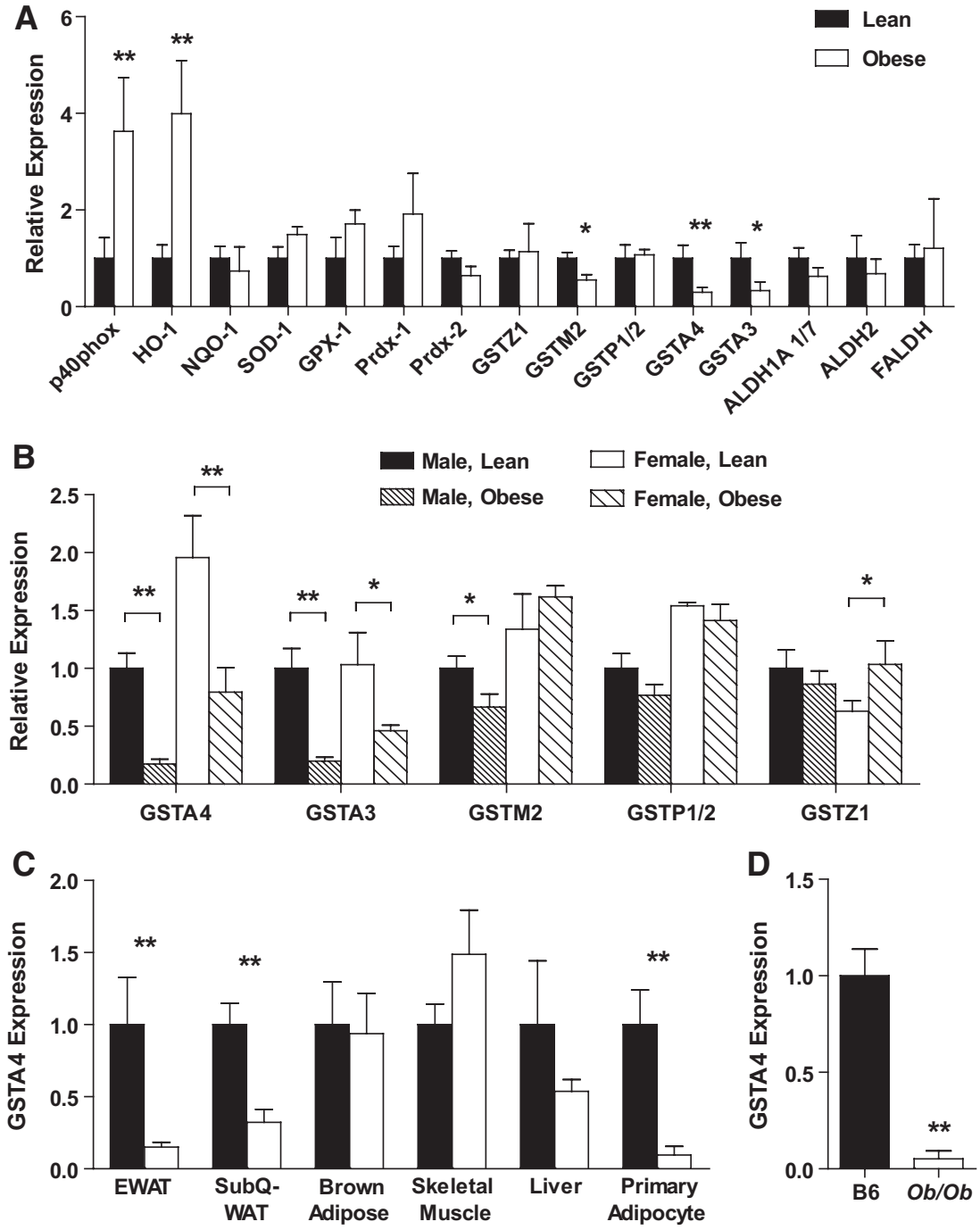

FIG. 1. Expression of oxidative stress–responsive genes in adipose tissue in obesity. C57BL/6J mice were fed either a low-fat or high-fat diet for 9–12 weeks, and mRNA was isolated from the indicated tissue. *A*: Expression of the indicated genes in epididymal WAT analyzed by qPCR (lean, $n = 8$; obese, $n = 7$). NQO-1, NADPH quninone oxidoreductase 1. *B*: Expression of GST isozymes in WAT of lean and obese male and female mice (male, lean, $n = 8$; male, obese, $n = 7$; female, lean, $n = 5$; female, obese, $n = 4$). *C*: Expression of GSTA4 in various tissues or cells from lean and obese male mice ($n = 8$). *D*: Expression of GSTA4 in C57BL/6J mice (B6) relative to that in adipose tissue of *ob/ob* mice. TBP, TATA-box binding protein; TFIIE, transcription factor II E. *$P < 0.05$; **$P < 0.01$.

shown). Moreover, the decrease in GSTA4 mRNA was evident in both the subcutaneous and omental fat depots. There was no correlation between GSTA4 expression and BMI (Fig. 3*B*), but there was a statistically significant negative correlation between GSTA4 levels and homeostatic model assessment of insulin resistance (HOMA-IR) (Fig. 3*C*). Evaluation of GSTA3 expression revealed no relationship to HOMA-IR or BMI (results not shown).

Generation of GSTA4-silenced adipocytes. Because GSTA4 is central to 4-HNE detoxification and metabolism and carbonylation is increased with obesity (15,26), we evaluated whether decreased GSTA4 expression leads directly to increased protein carbonylation. To that end, 3T3-L1 fibroblasts were transduced with shRNA directed against GSTA4 mRNA or nonspecific scrambled control sequence to establish GSTA4 knockdown and Scr cell lines. Although several distinct shRNA sequences were analyzed for GSTA4 silencing, one line with ~60–70% decrease in GSTA4, comparable with that observed in the animal system, was chosen for detailed assessment (Fig.

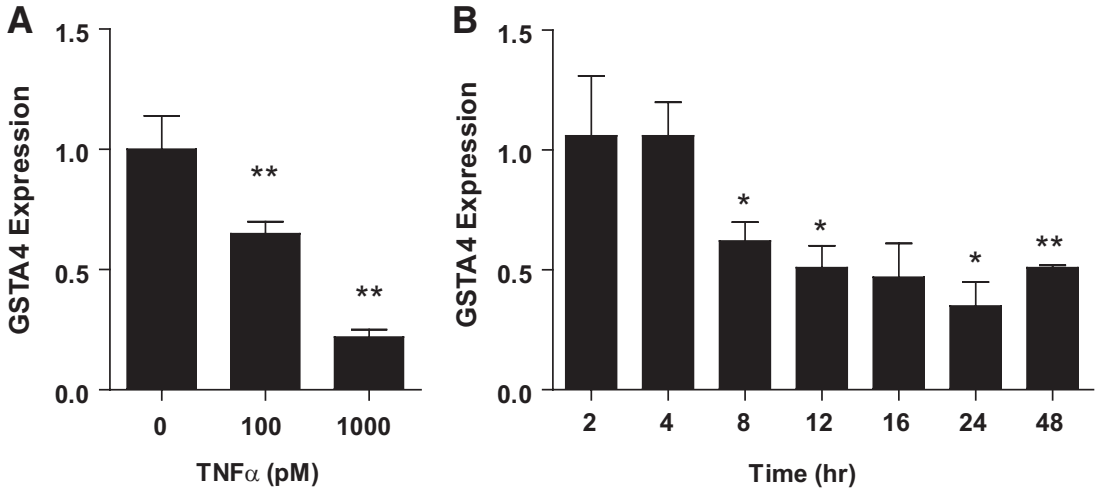

FIG. 2. Effect of TNF-α treatment on GSTA4 expression in 3T3–L1 adipocytes. qPCR analysis of GSTA4 mRNA expression in day-8 3T3–L1 adipocytes normalized to TFIIE as a function of (*A*) TNF-α level after 24 h or (*B*) time of treatment with 1 nmol/l TNF-α. *$P < 0.05$; **$P < 0.01$ relative to control samples.

4*A*); some measures were confirmed in other silenced cell lines. Although GSTA3 was not expressed in the preadipocytes at an appreciable level, its expression increased during preadipocyte differentiation (data not shown) and was upregulated approximately twofold in GSTA4 knockdown adipocytes compared with Scr adipocytes (Fig. 4*A*).

GSTA4 knockdown 3T3-L1 cells differentiated normally and expressed adipocyte marker proteins peroxisome proliferator–activated receptor-γ (PPARγ), CCAAT/enhancer binding protein α (CEBPα), adipocyte fatty acid–binding protein (A-FABP/aP2), β-actin, and lipoprotein lipase (LPL) to the same extent as Scr cells. Interestingly, expression of the fatty acid translocase CD36 was upregulated approximately twofold in the GSTA4 knockdown adipocytes (Figs. 4*B*).

Protein carbonylation in GSTA4 knockdown and Scr control cells was assessed by biotin hydrazide modification (Fig. 4*C*) (15). Adipocytes exhibited an approximately threefold to fourfold increase ($P < 0.01$) in total protein carbonylation relative to preadipocytes for both GSTA4 knockdown and Scr cell lines ($n = 4$). Increased carbonylation of specific proteins was noted in GSTA4 knockdown relative to Scr control adipocytes. The prominent band near ~15 kDa in adipocytes has previously been identified as the adipocyte fatty acid–binding protein (aP2) (15). Another protein at ~145 kDa (**) exhibited an approximately twofold to threefold increase ($P < 0.01$) in carbonylation in the GSTA4 knockdown cells. This band was excised from the gel and digested with trypsin, and the peptides were sequenced by liquid chromatography–electrospray ionization tandem mass spectrometry. The resultant peptides (nine unique peptides representing 8% sequence coverage) identified the protein as xanthine dehydrogenase (supplementary Table 2).

Altered glucose and lipid metabolism in GSTA4-silenced adipocytes. To determine the influence of increased protein carbonylation on adipocyte function, we examined a variety of metabolic parameters linked to glucose and lipid metabolism. GSTA4 knockdown adipocytes exhibited a significant increase in basal glucose transport, resulting in a net decrease in insulin-stimulated hexose uptake (Fig. 5*A* and *B*). Western analysis indicated increased expression of the basal GLUT, GLUT1 (Fig. 5*C*), but not the insulin-responsive GLUT, GLUT4. Consistent with increased hexose metabolism, analysis of reduced coenzyme levels revealed that the ratio of NAD^+/NADH was significantly lower in GSTA4 knockdown cells (Fig. 5*D*) and the culture medium of GSTA4 knockdown cells was slightly acidic (results not shown) due to a 65–70%

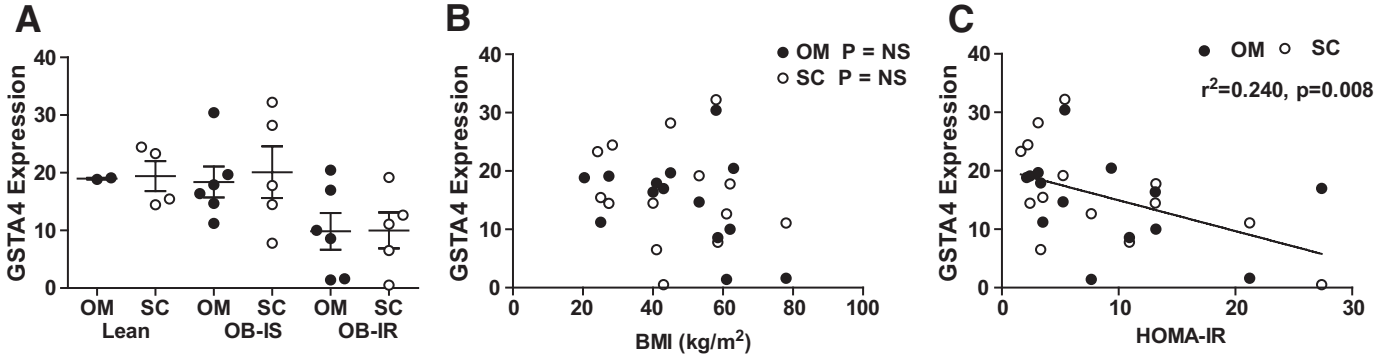

FIG. 3. Expression of human GSTA4 in obesity and insulin resistance. *A*: Relative expression of GSTA4 in omental and subcutaneous white adipose tissues of patients characterized as lean insulin sensitive (Lean), obese insulin sensitive (OB-IS), or obese insulin resistant (OB-IR). Data are expressed using means ± SEM. *B*: Correlation of GSTA4 mRNA expression in omental or subcutaneous adipose with patient BMI in kg/m^2. *C*: Correlation of GSTA4 mRNA expression in omental or subcutaneous adipose with HOMA-IR, calculated as [insulin (μU/ml) × glucose (mmol/l)]/22.5. Each data point represents one individual.

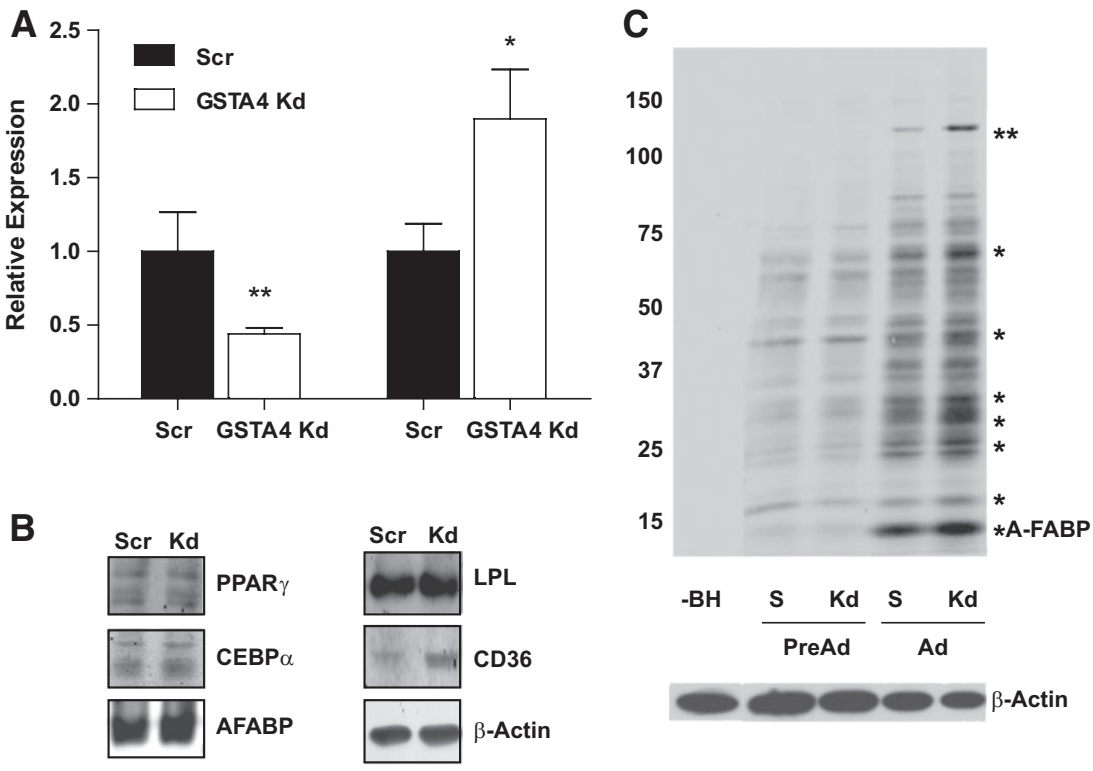

FIG. 4. GSTA4 silencing and protein carbonylation in 3T3–L1 adipocytes. *A*: Relative levels of GSTA4 and GSTA3 mRNA were quantified by qPCR (n = 6 per group). GSTA4 expression was normalized to TFIIE, and GSTA3 expression was normalized to 36B4. *B*: Expression of adipogenic marker proteins (n = 6 per group). *C*: Protein carbonylation in GSTA4 knockdown and Scr control cells. Protein bands found to have increased carbonylation in the GSTA4 knockdown adipocytes are indicated (*). The ~145-kDa band (**) was digested and subjected to liquid chromatography–electrospray ionization tandem mass spectrometry for protein identification detailed in supplementary Table 2. S, scrambled, −BH, minus biotin hydrazide. *C*: A composite in which the −BH lane has been moved from the same digital image (at the same exposure) to be adjacent to the experimental lanes.

increased level of L(+)-lactate compared with scrambled control cells (Fig. 5*E*).

Because tricarboxylic acid cycle (TCA) enzymes are targets of protein carbonylation and are inactivated by the addition of 4-HNE (27,28), GSTA4 knockdown and Scr adipocytes were assayed for small organic acids by direct injection tandem mass spectrometry (29). GSTA4 knockdown adipocytes had significantly increased ($P < 0.01$) levels of intracellular lactate, pyruvate, succinate, and citrate (Fig. 5*F*). The ratio of lactate to pyruvate was also significantly decreased in GSTA4 knockdown adipocytes relative to Scr control cells, and in sum suggested that multiple steps in the tricarboxylic acid cycle may be compromised because of silencing of GSTA4 and increased protein carbonylation.

To profile lipid metabolism in GSTA4-silenced 3T3-L1 adipocytes, we evaluated ^{14}C-acetate incorporation into lipid pools as a measure of de novo lipogenesis. GSTA4 knockdown adipocytes exhibited no difference in de novo lipogenesis under basal or insulin-stimulated conditions relative to scrambled control cells (results not shown). However, consistent with elevated CD36 expression (Fig. 4*B*), fatty acid uptake measured by ^{3}H-palmitate influx was slightly, but significantly, increased under basal (but not insulin-stimulated) conditions in GSTA4 knockdown adipocytes (results not shown). Although both basal glucose and fatty acid transport are increased in GSTA4 knockdown cells, total lipid storage was unchanged. We therefore analyzed lipolysis of nonesterified fatty acids from GSTA4 knockdown and Scr adipocytes. Silencing GSTA4 led to an ~50% increase in basal lipolysis, even in the presence of insulin (Fig. 5*G*). Insulin suppression of forskolin-stimulated lipolysis was slightly blunted in GSTA4 knockdown adipocytes (Fig. 5*H*). These results were confirmed in separate GSTA4 knockdown 3T3-L1 cell lines generated from different shRNA sequences (data not shown).

To assess mitochondrial β-oxidation, the conversion of radiolabeled palmitate to CO_2 and soluble metabolites was evaluated (30). GSTA4 knockdown adipocytes exhibited decreased oxidation of [1-^{14}C]-palmitate as determined by the production of ^{14}C-labeled CO_2 (complete oxidation) and ^{14}C-labeled acid-soluble metabolites (incomplete oxidation) (Fig. 5*I*). Mass spectrometry–based analyses were used to detect changes in the acyl-carnitine profile of GSTA4-silenced adipocytes (supplementary Fig. 1) and revealed that acetyl-carnitine (C2) and several other long-chain acyl-carnitine species were elevated in GSTA4 knockdown cells.

Silencing of GSTA4 expression leads to impaired respiration. Given the altered glucose metabolism and TCA cycle intermediates, we assessed mitochondrial respiration in GSTA4 knockdown and control cells. Mitochondria were isolated from GSTA4 knockdown and Scr adipocytes, and oxygen consumption was evaluated. GSTA4 silencing had a significant effect ($P = 0.017$) on oxygen consumption rate as assessed by two-way ANOVA with Bonferroni post hoc analysis. Whereas control 3T3-L1 adipocytes exhibited robust state 2 respiration and an increase in state 3 respiration after addition of ADP, GSTA4 knockdown mitochondria displayed approximately twofold decrease in state 2 respiration and no increase in

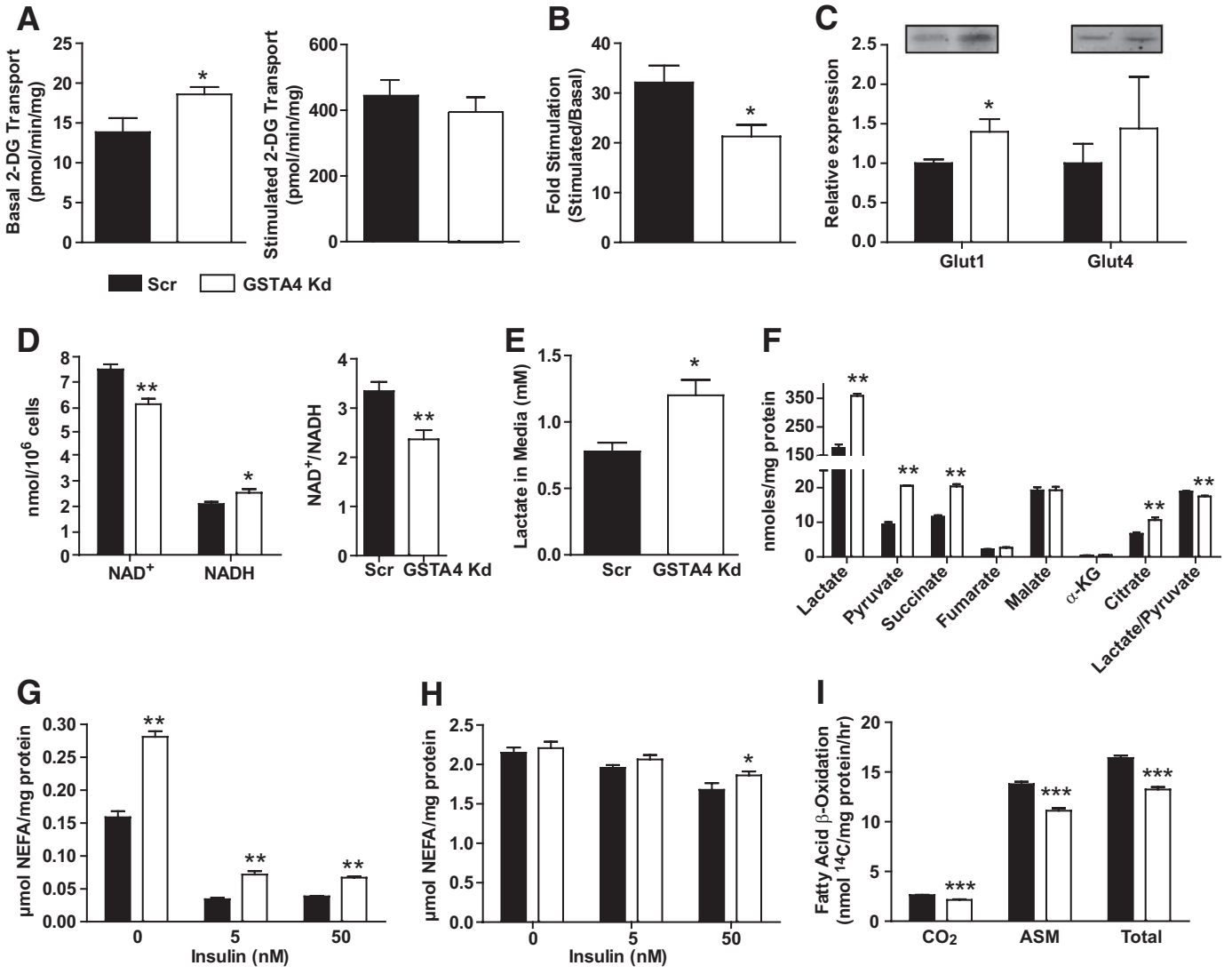

FIG. 5. Glucose and lipid metabolism in GSTA4 knockdown and Scr adipocytes. *A*: Transport of 2-deoxyglucose (2-DG) in GSTA4 knockdown and Scr adipocytes under basal (left) and 100 nmol/l insulin-stimulated (right) conditions. *B*: Fold stimulation of hexose transport in GSTA4 knockdown and Scr 3T3–L1 adipocytes ($n = 9$). *C*: Expression of glucose transporters GLUT1 and GLUT4 ($n = 6$ per group). *D*: NAD^+, NADH, and NAD^+/NADH in day 7 GSTA4 knockdown and Scr adipocytes ($n = 6$). *E*: L(+)-lactate in the medium of GSTA4 knockdown and Scr cells ($n = 6$). *F*: Organic acids from GSTA4 knockdown and Scr adipocyte cell lysates. Basal (*G*) and forskolin-stimulated (*H*) lipolysis in Scr and GSTA4 knockdown 3T3–L1 adipocytes. *I*: β-oxidation of [^{14}C]-palmitate in Scr and knockdown adipocytes ($n = 6$). *G* and *H*: Analyzed by two-way ANOVA with Bonferroni post hoc analysis. *$P < 0.05$; **$P < 0.01$.

oxygen consumption after addition of ADP (Fig. 6*A*–*C*). As mitochondrial dysfunction is often coupled with increased reactive oxygen species generation, we evaluated superoxide anion production in isolated mitochondria (21). Silencing GSTA4 resulted in an approximately threefold increase in superoxide production in the mitochondrial matrix (Fig. 6*D*). However, whole-cell ROS evaluated by the fluorescent probe chloromethyl 2′,7′-dichlorodihydrofluorescein diacetate (H_2DCFDA) was not changed in GSTA4 knockdown compared with Scr control cells (data not shown), suggesting that increased oxidative stress is centered on the mitochondrion and not a property of the entire cell.

In the muscle, insulin resistance is characterized by not only loss of mitochondrial function but also mitochondria protein and DNA, leading to reduced levels of functional organelles (31,32). As such, we evaluated markers of mitochondrial biogenesis at the mRNA, protein, and DNA level. The expression of the key transcription factors Nrf1 and Tfam as well as the central cofactor peroxisome proliferator–activated γ coactivator-1α (PGC-1α) are all reduced in GSTA4-silenced adipocytes as well as the expression of mitochondrial proteins cyclooxygenase IV (COX IV) and cytochrome c (Fig. 7*A* and *B*). Interestingly, expression of manganese SOD (Mn-SOD) and uncoupling protein 2 (UCP2) was not affected by GSTA4 silencing. In the GSTA4 knockdown cells, endothelial NO synthase (eNOS) expression was downregulated ~50%, suggesting that increased protein carbonylation initiates a cascade of events that links to the entire mitochondrial biogenesis pathway (32). Consistent with this, the abundance of the COX II and cytochrome b (mitochondrial) genes relative to UCP2 (nuclear) gene was significantly reduced (Fig. 7*C*). Paralleling the reduction in state 3 respiration, Fig. 7*D* shows that the activity of ATP synthase was reduced 50% in the GSTA4-silenced adipocytes.

To determine whether mitochondrial dysfunction in the GSTA4-silenced 3T3-L1 cells was also exhibited in animal

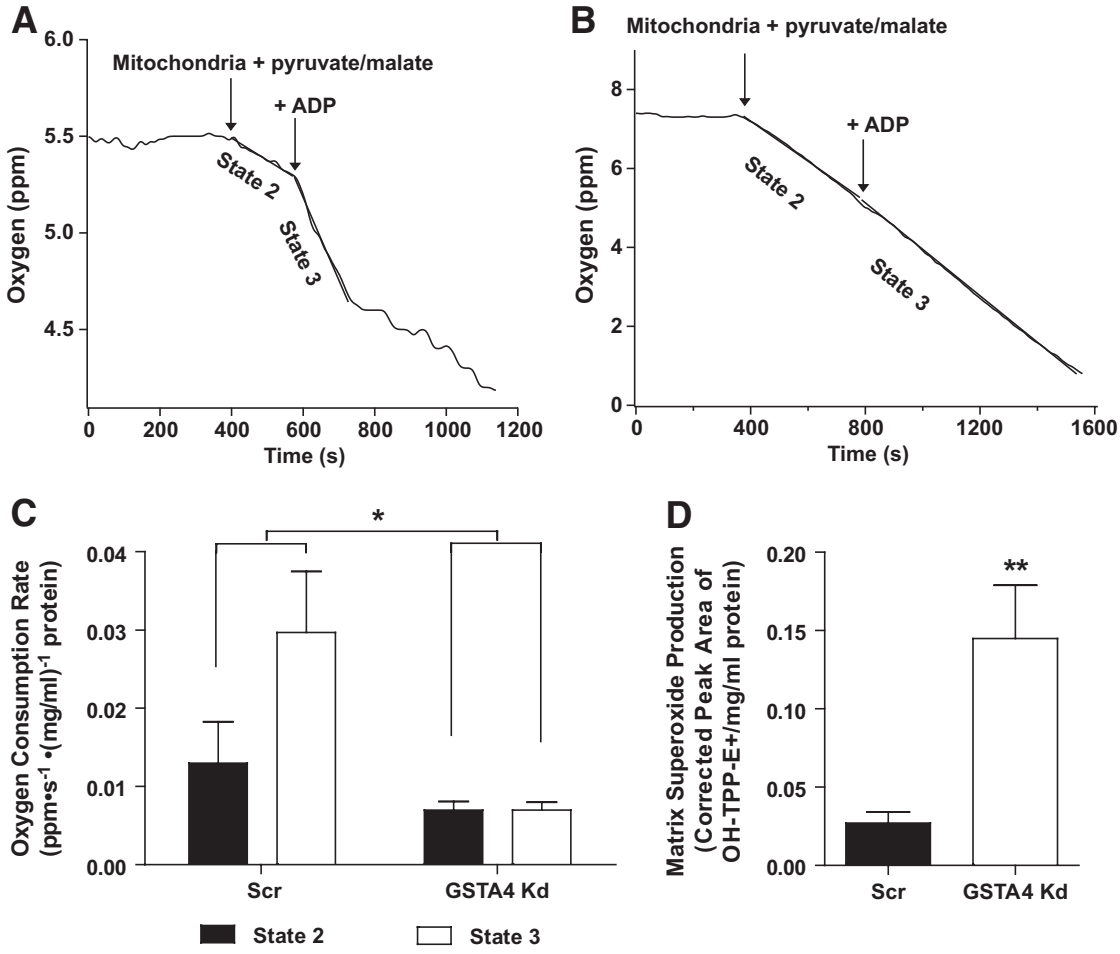

FIG. 6. Mitochondria function in GSTA4 knockdown and Scr 3T3–L1 adipocytes. Mitochondrial oxygen consumption in Scr (*A*) or GSTA4 knockdown (*B*) adipocytes. *C*: Oxygen consumption rates for Scr and GSTA4 knockdown adipocytes ($n = 3$). Statistics calculated by two-way analysis with Bonferroni post hoc analysis. *D*: Mitochondrial matrix superoxide production in GSTA4 knockdown and Scr adipocytes ($n = 3$).

systems, respiration was evaluated in mitochondria isolated from male GSTA4-null (−/−) mice and wild-type (+/+) littermates maintained on standard chow (lean) or high-fat (obese) diet. Lean or obese GSTA4-null mice exhibited no significant difference in body weight relative to wild-type controls (34.2 ± 3.3 g vs. 38.6 ± 4.0, chow diet; 45.6 ± 6.9 and 49.2 ± 9.0, high-fat diet). No changes in fasting glucose or insulin levels were found between wild-type and GSTA4-null mice (supplementary Fig. 2*B*). Figure 8*A* and *B* show that in wild-type C57BL/6J mice, the lean to obese transition results in little change in state 2 respiration but a decrease in state 3 respiration, coincident with the downregulation of GSTA4. Interestingly, GSTA4-null mice exhibited a trend toward increased state 2 respiration relative to wild-type animals. The state 3 oxygen consumption rate of mitochondria from lean GSTA4-null mice was comparable with wild type; however, similar to mitochondria from GSTA4-silenced adipocytes, mitochondria from obese GSTA4-null mice displayed no increase in oxygen consumption in response to ADP.

Accompanying the changes in respiration, adipocyte mitochondria from wild-type mice produced twofold to threefold more matrix superoxide in the obese state compared with lean controls. Adipocyte mitochondria from GSTA4-null mice exhibited markedly increased matrix superoxide in the lean state compared with wild-type controls and an even greater level of superoxide in the obese state (Fig. 8*C*). These findings are consistent with published reports that defects in oxidative phosphorylation lead to increased matrix superoxide (33) and are likely a consequence of elevated protein carbonylation in the mitochondria of EWAT from GSTA4-null mice (Fig. 8*D*). Unlike the GSTA3 upregulation in GSTA4 knockdown 3T3-L1 cell culture model, there was no significant change in expression of GSTA3 or other glutathione S-transferases or dehydrogenases linked to 4-HNE metabolism in the GSTA4-null mice (supplementary Fig. 2*A*).

DISCUSSION

The work described here profiles the systemic metabolic events associated with downregulation of GSTA4 that initiate with carbonylation of cellular proteins. Protein carbonylation is a chemical event with multiple protein targets alkylated under conditions of increased oxidative stress, and the biological outcomes in a cell or tissue are not likely to be based solely on one specific protein modification event (34). As such, a systems-wide approach is needed to characterize functional consequences of carbonylation. Our previous work characterized carbonylated polypeptides in adipose tissue using proteomic methods (15), and this report extends those findings to metabolic outcomes. The results presented identify

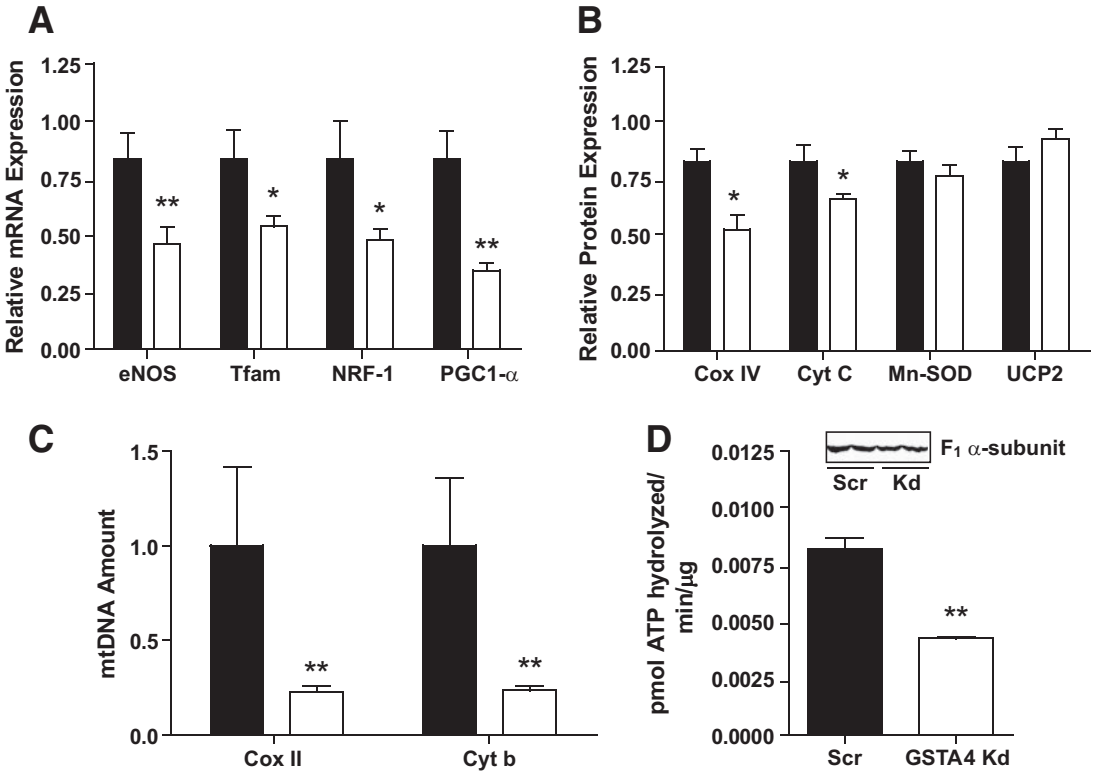

FIG. 7. Expression of genes and proteins linked to mitochondrial biogenesis. *A*: Expression of transcription factors and target mRNA in GSTA4-silenced (open bars) and scrambled (closed bars) adipocytes ($n = 6$). *B*: Mitochondrial protein expression in GSTA4 knockdown and Scr adipocytes ($n = 3$–6). *C*: Expression of COX II and cytochrome b DNA relative to UCP2 DNA in GSTA4 knockdown and Scr adipocytes ($n = 6$). *D*: Activity of ATP synthase in GSTA4-silenced and scrambled adipocytes and level of ATP synthase α-subunit protein ($n = 3$). *$P < 0.05$; **$P < 0.01$.

GSTA4 as a key determinant of adipocyte protein carbonylation and mitochondrial function and suggest that its activity may be a protective factor against metabolic dysfunction.

In humans, GSTA4 is downregulated in omental and subcutaneous depots of obese, insulin-resistant but not obese, insulin-sensitive individuals (Fig. 3). Similarly, GSTA4 is downregulated specifically in adipose tissue from obese, insulin-resistant C57BL/6J mice (15,24), in *ob/ob* animals (Fig. 1*D*), or in TNF-α–treated 3T3-L1 adipocytes (Fig. 2). Previous work by Awasthi et al. (11) and Engle et al. (35) has shown GSTA4-null mice have increased levels of 4-HNE, reduced antioxidant capacity, and increased apoptosis. Although GSTA4 expression was downregulated in obese female mice, its basal expression was more robust than in males (Fig. 1*B*), raising the possibility that increased levels of GSTA4 protect female mice from the harmful effects of lipid peroxidation products and may contribute to the attenuated insulin resistance characteristics observed in female C57BL/6J mice (36).

Although silencing GSTA4 in adipocytes also led to overall increased protein carbonylation, one protein target identified was xanthine dehydrogenase (Fig. 3*D*). In vitro, xanthine dehydrogenase is converted from its dehydrogenase form to its oxidoreductase form by modification of cysteine residues (37). Such modification of xanthine dehydrogenase by 4-HNE or other lipid aldehydes could lead to an increased oxidoreductase activity of the enzyme and the production of superoxide anion, amplifying oxidative stress signaling. Interestingly, xanthine dehydrogenase is known to be converted to xanthine oxidoreductase in response to mitochondrial damage in vivo (38), providing a link between mitochondrial dysfunction and oxidative stress.

Consistent with elevated lactate, the increased basal glucose transport by GSTA4 knockdown adipocytes could be a compensatory response to diminished mitochondrial function. In muscle cells, mitochondrial dysfunction has previously been linked to increased basal glucose transport (39), and obese human type 2 diabetic patients also exhibit increased basal 2-deoxyglucose transport in skeletal muscle cells (20,40). Increased GLUT1 expression in GSTA4 knockdown adipocytes (Fig. 5*C*) is consistent with previous reports of increased glucose transport via GLUT1 during treatment of epithelial cells with inhibitors of mitochondrial oxidative phosphorylation (41) as well as reports of oxidative stress–induced increases in basal glucose transport in adipocytes (3). Increased basal glucose transport may provide sufficient ATP for metabolism and signaling because the levels of total and phospho–AMP-activated protein kinase were not altered in the GSTA4-silenced adipocytes (data not shown).

Insulin resistance is correlated with increased basal lipolysis (42), and GSTA4 knockdown adipocytes exhibited ~50% increased basal lipolysis in the presence or absence of insulin (Fig. 5*G*). Surprisingly, GSTA4 knockdown adipocytes had no change in total triglyceride accumulation (results not shown), potentially because of increased fatty acid uptake. Consistent with this, the expression of CD36 protein, a plasma membrane fatty acid transporter whose expression is induced by the 4-HNE–responsive transcription factor Nrf2 (43), was significantly increased in the GSTA4 knockdown adipocytes (Fig. 4*B*).

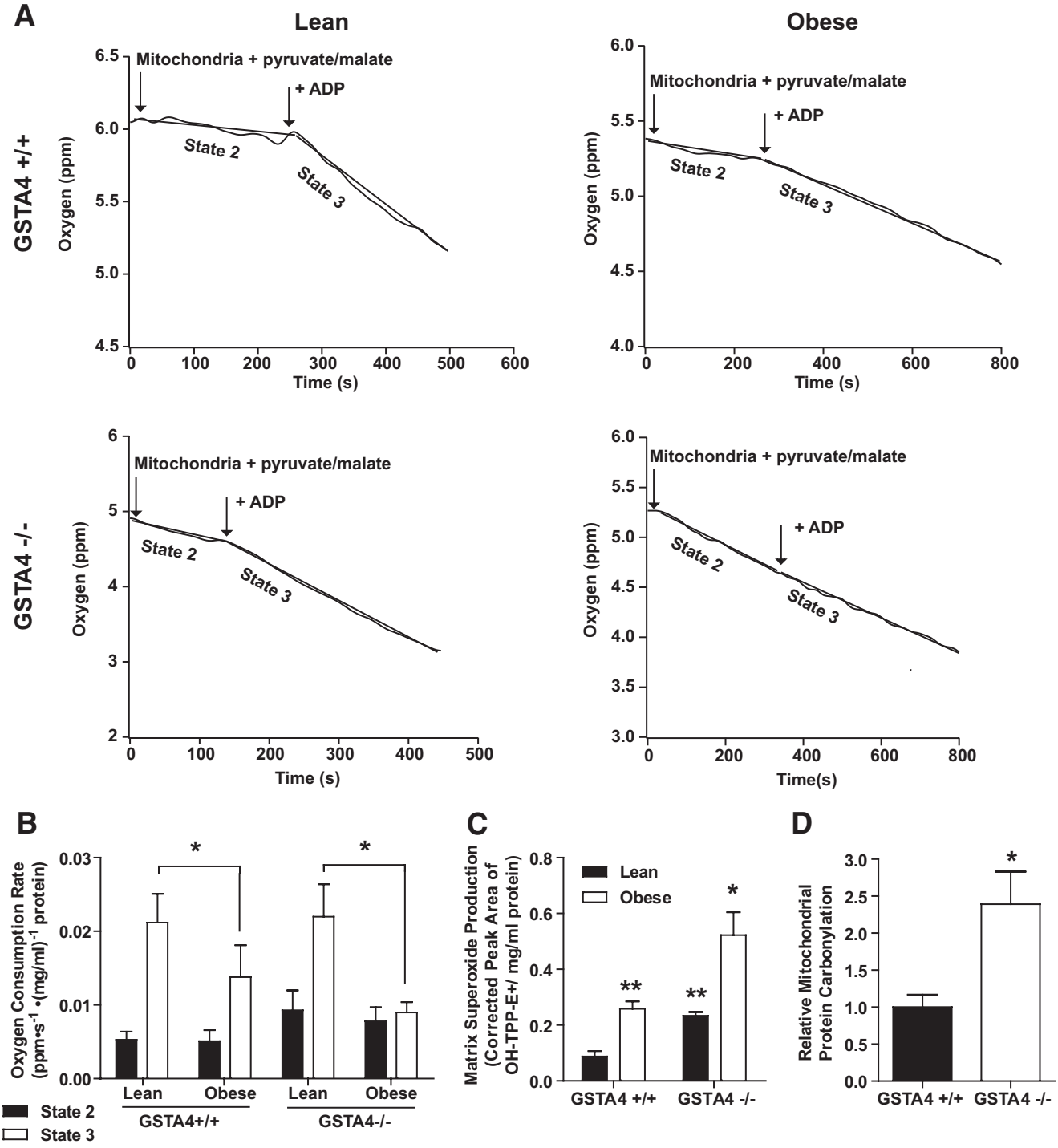

FIG. 8. Mitochondrial function and expression in adipose tissue from C57BL/6J and GSTA4-null (−/−) mice. Mitochondria were isolated from EWAT of 4- to 5-month-old mice maintained on a standard chow (lean) or high-fat (obese) diets. *A*: Mitochondrial oxygen consumption in lean and obese wild-type (+/+) and GSTA4-null (−/−) adipose. The mitochondrial protein concentrations were 0.22 (lean +/+), 0.23 (obese +/+), 0.20 (lean −/−), and 0.23 (obese −/−) mg/ml. *B*: Oxygen consumption rates for all four groups ($n = 3$). Statistics calculated using two-way ANOVA for each state with Holm-Sidak post hoc analysis. Variation due to loss of GSTA4 in state 2: $P = 0.1$; variation due to obesity in state 3: $P = 0.03$. *C*: Mitochondrial matrix superoxide production ($n = 3$). Statistics calculated using two-way ANOVA with Bonferroni post hoc analysis. Effect of obesity: $P = 0.0009$; effect of GSTA4: $P = 0.0018$. *D*: Quantitation of mitochondrial protein carbonylation in EWAT from lean wild-type and GSTA4-null mice ($n = 6$). *$P < 0.05$, **$P < 0.01$, ***$P < 0.001$.

The increase in key organic anion intermediates suggests that the flux through the tricarboxylic acid cycle is attenuated. Previous proteomic data have identified multiple TCA cycle enzymes as well as complexes I–IV of the oxidative phosphorylation machinery as targets of carbonylation (34). The decrease in [1-^{14}C]-palmitate oxidation (Fig. 5*I*) indicates that multiple steps in lipid oxidation and/or metabolism of acetyl-CoA are reduced in the GSTA4-silenced cells. This is supported by mass spectrometry data that show elevated levels of several acyl-carnitine species (supplementary Fig. 1), and increased acetyl-carnitine suggests that acetyl-CoA is accu-

mulating. As such, increased protein carbonylation in the mitochondrion is likely to lead to decreased functions such as tricarboxylic acid cycle and fatty acid oxidation (27,44).

A major finding of this study is that respiration is markedly altered in GSTA4 knockdown adipocytes (Fig. 6) and in adipocytes of both lean and obese GSTA4-null mice (Fig. 8). In the cell culture system, silencing of GSTA4 led to diminished oxygen consumption (Fig. 6*C*) and increased NADH levels (Fig. 5*D*), suggesting electron transfer through the electron transport chain is impaired. Moreover, there was no increase in oxygen consumption in response to ADP in mitochondria from the GSTA4-silenced adipocytes. Consistent with this, the activity of ATP synthase was decreased ~50% in the GSTA4-silenced adipocytes. These observations may be due to a combination of factors, including increased proton leakage across the inner mitochondrial membrane, carbonylation of complex V proteins affecting the ability to couple the proton gradient to ATP production, the carbonylation of the adenine nucleotide translocator, or carbonylation-dependent changes in the abundance of critical proteins linked to state 3 respiration. Indeed, under certain conditions 4-HNE can facilitate proton leak in other cell types through adenine nucleotide translocator or uncoupling proteins (45,46).

In the GSTA4-null adipocytes, changes in both state 2 and state 3 respiration were similar but not identical to the 3T3-L1 GSTA4 knockdown system. In the animal model, mitochondria from lean wild-type C57BL/6J mice exhibit robust state 2 respiration that increased with the addition of ADP. Obese C57BL/6J mice exhibited no change in state 2 respiration relative to lean counterparts but had attenuated ADP-coupled oxygen consumption, potentially due to the downregulation of GSTA4. In GSTA4-null animals, mitochondria from lean and obese mice exhibited a trend toward increased state 2 respiration compared with the wild-type animals, possibly due to increased proton leakage. Indeed, previous studies by Echtay et al. (45) have suggested that carbonylation of uncoupling proteins may, under certain circumstances, lead to increased proton leak, thereby providing for increased state 2 respiration. Similar to the GSTA4-silenced cells, mitochondria from obese GSTA4-null mice exhibited virtually no increase in respiration with ADP (Fig. 8*A* and *B*).

Associated with downregulation of GSTA4 is decreased expression of eNOS, Nrf1, PGC-1α, and Tfam, critical regulators of mitochondrial biogenesis (Fig. 7). Indeed, GSTA4-silencing resulted in loss of mitochondrial DNA and decreased expression of COX II and cytochrome c. Work by Nisoli and colleagues has focused on eNOS as the key regulator of TNF-α action (32) and determined that if eNOS activity is lost from adipocytes, the entire program of mitochondrial activation and biogenesis is affected (47). These data suggest that downregulation of GSTA4 is upstream of eNOS regulation and may be mechanistically regulated by protein carbonylation.

In sum, the results presented here focus on the role of GSTA4 as an antioxidant enzyme responsible primarily for elimination of reactive electrophiles from adipocytes. The results here suggest a model whereby downregulation of GSTA4 by proinflammatory cytokines results in increased protein carbonylation, altered glucose and lipid metabolism, decreased mitochondrial β-oxidation, TCA cycle activity, electron transport, and respiration. Thus, protein carbonylation in white adipose tissue may provide a molecular mechanism linking increased oxidative stress to metabolic dysfunction associated with insulin resistance.

ACKNOWLEDGMENTS

This work was supported by National Institutes of Health (NIH) Grant DK-084669 to D.A.B., the Minnesota Obesity Center (NIH Grant DK-050456), and NIH National Heart, Lung, and Blood Institute Training Grant T32 HL-07741 to P.A.G.

No potential conflicts of interest relevant to this article were reported.

We thank the members of the Bernlohr research group who provided helpful suggestions regarding this work. We also thank Erik Refsland of the Minnesota Obesity Center for lentivirus production, Dr. Jason Fowler for assistance with studies using TNF-α, Dr. Bruce Witthuhn of the University of Minnesota Center for Mass Spectrometry and Proteomics for assistance with mass spectrometry, Dr. Stephen Katz for help with statistical analysis, and the Minnesota Supercomputing Institute for support in data analysis.

REFERENCES

1. Ogden CL, Carroll MD, Curtin LR, McDowell MA, Tabak CJ, Flegal KM. Prevalence of overweight and obesity in the United States, 1999–2004. JAMA 2006;295:1549–1555
2. Furukawa S, Fujita T, Shimabukuro M, Iwaki M, Yamada Y, Nakajima Y, Nakayama O, Makishima M, Matsuda M, Shimomura I. Increased oxidative stress in obesity and its impact on metabolic syndrome. J Clin Invest 2004;114:1752–1761
3. Talior I, Yarkoni M, Bashan N, Eldar-Finkelman H. Increased glucose uptake promotes oxidative stress and PKC-delta activation in adipocytes of obese, insulin-resistant mice. Am J Physiol Endocrinol Metab 2003;285: E295–E302
4. Anderson EJ, Lustig ME, Boyle KE, Woodlief TL, Kane DA, Lin CT, Price JW III, Kang L, Rabinovitch PS, Szeto HH, Houmard JA, Cortright RN, Wasserman DH, Neufer PD. Mitochondrial H2O2 emission and cellular redox state link excess fat intake to insulin resistance in both rodents and humans. J Clin Invest. 2009 Feb 2. pii: 37048. doi: 10.1172/JCI37048. [Epub ahead of print]
5. Houstis N, Rosen ED, Lander ES. Reactive oxygen species have a causal role in multiple forms of insulin resistance. Nature 2006;440:944–948
6. Lin Y, Berg AH, Iyengar P, Lam TK, Giacca A, Combs TP, Rajala MW, Du X, Rollman B, Li W, Hawkins M, Barzilai N, Rhodes CJ, Fantus IG, Brownlee M, Scherer PE. The hyperglycemia-induced inflammatory response in adipocytes: the role of reactive oxygen species. J Biol Chem 2005;280:4617–4626
7. Soares AF, Guichardant M, Cozzone D, Bernoud-Hubac N, Bouzaïdi-Tiali N, Lagarde M, Géloën A. Effects of oxidative stress on adiponectin secretion and lactate production in 3T3–L1 adipocytes. Free Radic Biol Med 2005;38:882–889
8. Bays H, Mandarino L, DeFronzo RA. Role of the adipocyte, free fatty acids, and ectopic fat in pathogenesis of type 2 diabetes mellitus: peroxisomal proliferator-activated receptor agonists provide a rational therapeutic approach. J Clin Endocrinol Metab 2004;89:463–478
9. Zarković N, Zarković K, Schaur RJ, Stolc S, Schlag G, Redl H, Waeg G, Borović S, Loncarić I, Jurić G, Hlavka V. 4-Hydroxynonenal as a second messenger of free radicals and growth modifying factor. Life Sci 1999;65: 1901–1904
10. Sayre LM, Lin D, Yuan Q, Zhu X, Tang X. Protein adducts generated from products of lipid oxidation: focus on HNE and one. Drug Metab Rev 2006;38:651–675
11. Awasthi YC, Sharma R, Cheng JZ, Yang Y, Sharma A, Singhal SS, Awasthi S. Role of 4-hydroxynonenal in stress-mediated apoptosis signaling. Mol Aspects Med 2003;24:219–230
12. Ueda K, Ueyama T, Yoshida K, Kimura H, Ito T, Shimizu Y, Oka M, Tsuruo Y, Ichinose M. Adaptive HNE-Nrf2-HO-1 pathway against oxidative stress is associated with acute gastric mucosal lesions. Am J Physiol Gastrointest Liver Physiol 2008;295:G460–G469
13. Piantadosi CA, Suliman HB. Mitochondrial transcription factor A induction by redox activation of nuclear respiratory factor 1. J Biol Chem 2006;281: 324–333

14. Grimsrud PA, Xie H, Griffin TJ, Bernlohr DA. Oxidative stress and covalent modification of protein with bioactive aldehydes. J Biol Chem 2008;283:21837–21841
15. Grimsrud PA, Picklo MJ Sr, Griffin TJ, Bernlohr DA. Carbonylation of adipose proteins in obesity and insulin resistance: identification of adipocyte fatty acid-binding protein as a cellular target of 4-hydroxynonenal. Mol Cell Proteomics 2007;6:624–637
16. He NG, Singhal SS, Srivastava SK, Zimniak P, Awasthi YC, Awasthi S. Transfection of a 4-hydroxynonenal metabolizing glutathione S-transferase isozyme, mouse GSTA4–4, confers doxorubicin resistance to Chinese hamster ovary cells. Arch Biochem Biophys 1996;333:214–220
17. Surwit RS, Kuhn CM, Cochrane C, McCubbin JA, Feinglos MN. Diet-induced type II diabetes in C57BL/6J mice. Diabetes 1988;37:1163–1167
18. Malide D, Ramm G, Cushman SW, Slot JW. Immunoelectron microscopic evidence that GLUT4 translocation explains the stimulation of glucose transport in isolated rat white adipose cells. J Cell Sci 2000;113(Pt. 23):4203–4210
19. Lobo S, Wiczer BM, Smith AJ, Hall AM, Bernlohr DA. Fatty acid metabolism in adipocytes: functional analysis of fatty acid transport proteins 1 and 4. J Lipid Res 2007;48:609–620
20. Mogensen M, Sahlin K, Fernström M, Glintborg D, Vind BF, Beck-Nielsen H, Højlund K. Mitochondrial respiration is decreased in skeletal muscle of patients with type 2 diabetes. Diabetes 2007;56:1592–1599
21. Xu X, Arriaga EA. Qualitative determination of superoxide release at both sides of the mitochondrial inner membrane by capillary electrophoretic analysis of the oxidation products of triphenylphosphonium hydroethidine. Free Radic Biol Med 2009;46:905–913
22. MacLaren R, Cui W, Simard S, Cianflone K. Influence of obesity and insulin sensitivity on insulin signaling genes in human omental and subcutaneous adipose tissue. J Lipid Res 2008;49:308–323
23. Tusher VG, Tibshirani R, Chu G. Significance analysis of microarrays applied to the ionizing radiation response. Proc Natl Acad Sci U S A 2001;98:5116–5121
24. Moraes RC, Blondet A, Birkenkamp-Demtroeder K, Tirard J, Orntoft TF, Gertler A, Durand P, Naville D, Bégeot M. Study of the alteration of gene expression in adipose tissue of diet-induced obese mice by microarray and reverse transcription-polymerase chain reaction analyses. Endocrinology 2003;144:4773–4782
25. Keller MP, Choi Y, Wang P, Davis DB, Rabaglia ME, Oler AT, Stapleton DS, Argmann C, Schueler KL, Edwards S, Steinberg HA, Chaibub Neto E, Kleinhanz R, Turner S, Hellerstein MK, Schadt EE, Yandell BS, Kendziorski C, Attie AD. A gene expression network model of type 2 diabetes links cell cycle regulation in islets with diabetes susceptibility. Genome Res 2008;18:706–716
26. Hubatsch I, Ridderstrom M, Mannervik B. Human glutathione transferase A4–4: an alpha class enzyme with high catalytic efficiency in the conjugation of 4-hydroxynonenal and other genotoxic products of lipid peroxidation. Biochem J 1998;330(Pt. 1):175–179
27. Humphries KM, Szweda LI. Selective inactivation of alpha-ketoglutarate dehydrogenase and pyruvate dehydrogenase: reaction of lipoic acid with 4-hydroxy-2-nonenal. Biochemistry 1998;37:15835–15841
28. Yoo BS, Regnier FE. Proteomic analysis of carbonylated proteins in two-dimensional gel electrophoresis using avidin-fluorescein affinity staining. Electrophoresis 2004;25:1334–1341
29. Koves TR, Ussher JR, Noland RC, Slentz D, Mosedale M, Ilkayeva O, Bain J, Stevens R, Dyck JR, Newgard CB, Lopaschuk GD, Muoio DM. Mitochondrial overload and incomplete fatty acid oxidation contribute to skeletal muscle insulin resistance. Cell Metab 2008;7:45–56
30. Koves TR, Noland RC, Bates AL, Henes ST, Muoio DM, Cortright RN. Subsarcolemmal and intermyofibrillar mitochondria play distinct roles in regulating skeletal muscle fatty acid metabolism. Am J Physiol Cell Physiol 2005;288:C1074–C1082
31. Ritov VB, Menshikova EV, He J, Ferrell RE, Goodpaster BH, Kelley DE. Deficiency of subsarcolemmal mitochondria in obesity and type 2 diabetes. Diabetes 2005;54:8–14
32. Valerio A, Cardile A, Cozzi V, Bracale R, Tedesco L, Pisconti A, Palomba L, Cantoni O, Clementi E, Moncada S, Carruba MO, Nisoli E. TNF-alpha downregulates eNOS expression and mitochondrial biogenesis in fat and muscle of obese rodents. J Clin Invest 2006;116:2791–2798
33. Meany DL, Poe BG, Navratil M, Moraes CT, Arriaga EA. Superoxide released into the mitochondrial matrix. Free Radic Biol Med 2006;41:950–959
34. Meany DL, Xie H, Thompson LV, Arriaga EA, Griffin TJ. Identification of carbonylated proteins from enriched rat skeletal muscle mitochondria using affinity chromatography-stable isotope labeling and tandem mass spectrometry. Proteomics 2007;7:1150–1163
35. Engle MR, Singh SP, Czernik PJ, Gaddy D, Montague DC, Ceci JD, Yang Y, Awasthi S, Awasthi YC, Zimniak P. Physiological role of mGSTA4–4, a glutathione S-transferase metabolizing 4-hydroxynonenal: generation and analysis of mGsta4 null mouse. Toxicol Appl Pharmacol 2004;194:296–308
36. Gallou-Kabani C, Vige A, Gross MS, Rabes JP, Boileau C, Larue-Achagiotis C, Tome D, Jais JP, Junien C. C57BL/6J and A/J mice fed a high-fat diet delineate components of metabolic syndrome. Obesity (Silver Spring) 2007;15:1996–2005
37. Rasmussen JT, Rasmussen MS, Petersen TE. Cysteines involved in the interconversion between dehydrogenase and oxidase forms of bovine xanthine oxidoreductase. J Dairy Sci 2000;83:499–506
38. Saksela M, Lapatto R, Raivio KO. Irreversible conversion of xanthine dehydrogenase into xanthine oxidase by a mitochondrial protease. FEBS Lett 1999;443:117–120
39. Gaster M. Insulin resistance and the mitochondrial link: lessons from cultured human myotubes. Biochim Biophys Acta 2007;1772:755–765
40. Jackson S, Bagstaff SM, Lynn S, Yeaman SJ, Turnbull DM, Walker M. Decreased insulin responsiveness of glucose uptake in cultured human skeletal muscle cells from insulin-resistant nondiabetic relatives of type 2 diabetic families. Diabetes 2000;49:1169–1177
41. Hamrahian AH, Zhang JZ, Elkhairi FS, Prasad R, Ismail-Beigi F. Activation of Glut1 glucose transporter in response to inhibition of oxidative phosphorylation. Arch Biochem Biophys 1999;368:375–379
42. Arner P. Control of lipolysis and its relevance to development of obesity in man. Diabetes Metab Rev 1988;4:507–515
43. Ishii T, Itoh K, Ruiz E, Leake DS, Unoki H, Yamamoto M, Mann GE. Role of Nrf2 in the regulation of CD36 and stress protein expression in murine macrophages: activation by oxidatively modified LDL and 4-hydroxynonenal. Circ Res 2004;94:609–616
44. Humphries KM, Yoo Y, Szweda LI. Inhibition of NADH-linked mitochondrial respiration by 4-hydroxy-2-nonenal. Biochemistry 1998;37:552–557
45. Echtay KS, Esteves TC, Pakay JL, Jekabsons MB, Lambert AJ, Portero-Otín M, Pamplona R, Vidal-Puig AJ, Wang S, Roebuck SJ, Brand MD. A signalling role for 4-hydroxy-2-nonenal in regulation of mitochondrial uncoupling. EMBO J 2003;22:4103–4110
46. Vieira HL, Belzacq AS, Haouzi D, Bernassola F, Cohen I, Jacotot E, Ferri KF, El Hamel C, Bartle LM, Melino G, Brenner C, Goldmacher V, Kroemer G. The adenine nucleotide translocator: a target of nitric oxide, peroxynitrite, and 4-hydroxynonenal. Oncogene 2001;20:4305–4316
47. Tedesco L, Valerio A, Cervino C, Cardile A, Pagano C, Vettor R, Pasquali R, Carruba MO, Marsicano G, Lutz B, Pagotto U, Nisoli E. Cannabinoid type 1 receptor blockade promotes mitochondrial biogenesis through endothelial nitric oxide synthase expression in white adipocytes. Diabetes 2008;57:2028–2036